SPIE International Symposium

BiOS 2006
Biomedical Optics

21–26 January 2006   San Jose Convention Center • San Jose, California USA

Conferences • Courses • Exhibition

2006 Symposium Chairs

James Fujimoto, Massachusetts Institute of Technology

R. Rox Anderson, M.D., Wellman Center for Photomedicine, Massachusetts General Hospital and Harvard School of Medicine

Executive Organizing Committee:

Samuel Achilefu, Washington Univ.
Robert Alfano, CUNY/City College
Juanita Anders, USUHS
R. Rox Anderson, M.D., Wellman Center for Photomedicine, Massachusetts General Hospital and Harvard School of Medicine
Fred Azar, Siemens Corp Research
Lawrence Bass, M.D., New York Univ. Medical Ctr.
David Benaron, M.D., Spectros Corp.
Darryl Bornhop, Vanderbilt Univ.
Alexander Cartwright, SUNY/Univ. at Buffalo
Wei Chen, Univ. of Central Oklahoma
Bernard Choi, Univ. of California/Irvine
Carol Cogswell, Univ. of Colorado at Boulder
Gerald Cohn, Cyber Tech Applied Science
Jose-Angel Conchello, Oklahoma Medical Research Foundation
Gerard Coté, Texas A&M Univ.
Achilles Demetriou, M.D., Cedars-Sinai Medical Ctr.
Werner de Riese, M.D., Texas Tech Univ.
Jörg Enderlein, Forschungszentrum Jülich (Germany)
Daniel Farkas, Cedars-Sinai Medical Ctr.
Daniel Fried, Univ. of California/San Francisco
James Fujimoto, Massachusetts Institute of Technology
Israel Gannot, The George Washington Univ.
Kenton Gregory, M.D., Oregon Medical Laser Center

Warren Grundfest, M.D., Univ. of California/Los Angeles
Zygmunt Gryczynski, Univ. of Maryland/Baltimore
Michael Hamblin, Harvard Medical School
Henry Hirschberg, M.D., Rikshospitalet (Norway)
Arthur Ho, Univ. of New South Wales (Australia)
Justus Ilgner, M.D., Univ. Hospital Aachen (Germany)
Joseph Izatt, Duke Univ.
Steven Jacques, Oregon Health and Science Univ.
Thomas M. Jovin, M.D., Max Planck Institute for Biophysical Chemistry (Germany)
Alvin Katz, CUNY/City College
Abraham Katzir, Tel Aviv Univ. (Israel)
David Kessel, Wayne State Univ.
Nikiforos Kollias, M.D., Johnson & Johnson
Joseph Lakowicz, Univ. of Maryland/Baltimore
Robert Leif, Newport Instruments
Michael Lucroy, D.V.M., Purdue Univ.
Steen Madsen, Univ. of Nevada/Las Vegas
Anita Mahadevan-Jansen, Vanderbilt Univ.
Reza Malek, M.D., Mayo Clinic
Fabrice Manns, Univ. of Miami
Karen McNally-Heintzelman, Advent Surgical Innovations
Dan Nicolau, Swinburne Univ. of Technology (Australia)
Alexander Oraevsky, Fairway Medical Technologies

Marek Osiński, The Univ. of New Mexico
Ammasi Periasamy, Univ. of Virginia
Wolfgang Petrich, Roche Diagnostics GmbH (Germany)
Paras Prasad, SUNY/Univ. at Buffalo
Alexander Priezzhev, M.V. Lomonosov Moscow State Univ. (Russia)
Ramesh Raghavachari, U.S. Food and Drug Administration
Peter Rechmann, D.D.S., Univ. of California/San Francisco
William Roach, Air Force Research Lab.
Alexander Savitsky, Institute of Biochemistry (Russia)
Peter So, Massachusetts Institute of Technology
Per Söderberg, St. Erik's Eye Hospital (Sweden)
Lloyd Tate, V.D.M., North Carolina State Univ.
Guillermo Tearney, M.D., Harvard Medical School
Eugene Trowers, M.D., Florida State Univ.
Valery Tuchin, Saratov State Univ. (Russia)
Tuan Vo-Dinh, Oak Ridge National Lab.
Lihong Wang, Texas A&M Univ.
Thomas Wang, Stanford Univ.
Ronald Waynant, U.S. Food and Drug Administration
Tony Wilson, Univ. of Oxford (United Kingdom)
Brian Wong, M.D., Univ. of California/Irvine
Kenji Yamamoto, M.D., International Medical Ctr. of Japan and Univ. of Tokyo (Japan)
Haishan Zeng, BC Cancer Agency (Canada)

Program on
Biomedical Spectroscopy, Microscopy, and Imaging

Program Track Chair: **Ammasi Periasamy,** Univ. of Virginia

Saturday	Sunday	Monday	Tuesday	Wednesday	Thursday
21 January	22 January	23 January	24 January	25 January	26 January

Technical Conferences

Saturday	Sunday	Monday	Tuesday	Wednesday	Thursday
		6088 **Imaging, Manipulation, and Analysis of Biomolecules, Cells, and Tissues III** *(Farkas, Leif, Nicolau)* p. 50			
	6089 **Multiphoton Microscopy in the Biomedical Sciences VI** *(Periasamy, So)* p. 52			6090 **Three-Dimensional and Multidimensional Microscopy: Image Acquisition and Processing XIII** *(Conchello, Cogswell, Wilson)* p. 54	
6092 **Ultrasensitive and Single-Molecule Detection Technologies** *(Enderlein, Gryczynski)* p. 56			6091 **Optical Biopsy VI** *(Alfano, Katz)* p. 55		
6093 **Biomedical Vibrational Spectroscopy IV: Advances in Research and Industry** *(Mahadevan-Jansen, Petrich)* p. 57				6094 **Optical Diagnostics and Sensing VI** *(Coté, Priezzhev)* p. 59	

Related Courses

Saturday	Sunday	Monday	Tuesday	Wednesday	Thursday
	SC029 Tissue Optics (Jacques) 1:30 pm to 5:30 pm, p. 165	SC696 Bioluminescence for Food and Environmental Safety (Brovko) 8:30 am to 12:30 pm, p. 168	SC603 Laser Product Certification to National and International Regulations (Stoev) 8:30 am to 5:30 pm, p. 154	SC695 Noninvasive in vivo Biosensing Based on Color Fluorescent Proteins for Drug Design and Screening (Savitsky) 8:30 am to 5:30 pm, p. 168	
	SC309 Fluorescent Markers: Usage and Optical System Optimization (Levi) 8:30 am to 12:30 pm, p. 167	SC751 Vibrational Spectroscopy: From Physics to Medicine (Petrich) 1:30 pm to 5:30 pm, p.167		SC768 Optoacoustic Systems for Medical Imaging: From Principles to Clinical Applications (Oraevsky) 1:30 pm to 5:30 pm, p. 166	
	SC437 Microfabrication Techniques for MicroFluidics & BioMEMS (Madou) 1:30 pm to 5:30 pm, p. 160			SC769 Laser Safety: Principles and Accident Prevention (Barat) 8:30 am to 5:30 pm, p. 155	
	SC312 Principles and Applications of Optical Coherence Tomography (Fujimoto) 8:30 am to 12:30 pm, p. 166				
	SC461 Bio-Optical Detection Systems (Levi) 1:30 pm to 5:30 pm, p. 167				
	SC693 Spectral Imaging for Biology and Medicine (Mansfield, Levenson) 8:30 am to 12:30 pm, p. 166				
	SC746 Introduction to Ultrafast Technology (Trebino) 8:30 am to 12:30 pm, p. 157				
	SC749 Diffuse Optical Spectroscopy and Imaging of Tissues (Toronov) 8:30 am to 5:30 pm, p. 167				
	SC750 Optical Clearing of Tissue and Blood (Tuchin) 12:30 pm, p. 165				

Investigation of metallic nanowire-based localized surface plasmon resonance optical biosensors using extinction spectra

Kyung Min Byun[a], Sung June Kim[a], and Donghyun Kim[b]

[a]School of Electrical Engineering, Seoul National University, Seoul, Korea 151-742;
[b]School of Electrical and Electronic Engineering, Yonsei University, Seoul, Korea 120-749

ABSTRACT

In this study, we investigate the impact of the cross sectional profile of an array of metallic nanowires on the feasibility of a localized surface plasmons resonance (LSPR) biosensor. Calculations were performed using rigorous coupled wave analysis with an emphasis on the extinction properties of the LSPR structure. It was confirmed that the resonance spectrum strongly depends on the nanowire period and profile. Our numerical results indicate that the nanowire structure, particularly that of a T-profile, delivers extremely linear sensing performance over a wide range of target refractive index with much enhanced sensitivity. The extinction-based LSPR structure also involves relatively large dimension and thus is expected to provide a feasible biosensor using current semiconductor technology.

Keywords: Localized surface plasmon resonance, biosensors, nanowires, rigorous coupled wave analysis

1. INTRODUCTION

A surface plasmon resonance (SPR) biosensor is an optical device based on the excitation of surface plasmons, in which plasma oscillations in a metal film are excited by the incident light in the attenuated total reflection configuration to be used as a sensitivity indicator.[1,2,3,4,5] In the resonance condition, incident light energy is mostly absorbed as excited evanescent waves are coupled to binding analytes on a thin metal film. Since the reflectance curve exhibits a minimum at resonance, surface reactions of interest can be quantified by measuring the shift of the reflectance curve.

Surface plasmons can also be excited in metallic nanostructures. It has been well-known that noble metal nanostructures allow direct and strong optical coupling of the incident light to resonantly driven electron plasma oscillations, called localized surface plasmons (LSPs).[6] Metallic nanostructures, if significantly smaller than the light wavelength, show an intense optical absorption band in the visible range.[7] Compared to surface plasmon polaritons (SPPs) excited in a thin metal film, the LSP resonance (LSPR) excitation is characteristic of substantial enhancement of electromagnetic fields as a result of strong absorption and highly efficient light scattering.[8] These enhanced fields induce significantly high sensitivity to changes in the local environment caused by binding molecules surrounding the nanostructures.[9,10]

For this reason, many researchers have proposed SPR biosensing systems incorporating metallic nanostructures for various sensing applications.[11,12,13,14] Typical experiments involve gold or silver nanostructures deposited over a thin metal film to bind with specific target analytes and to excite the localized plasmons. The experimental results indicated that these modified sensing schemes improve sensitivity more than ten-times compared to a conventional SPR biosensor.[11,13] However, nanostructure-modified SPR biosensors have a fundamental constraint that SPP-LSP interactions can limit the effectiveness of excited LSP modes.[15]

Recently, regularly patterned metallic nanostructure arrays without a metal film on a dielectric substrate have drawn tremendous interests as a potential tool to implement biosensors.[16,17] This configuration is fully based on the LSP modes, thus its performance is not interfered by the SPP-LSP interactions. Unlike a biosensor based on SPP-LSP coupled modes, field enhancement is mostly associated with the coupling effects between resonant LSP modes that are excited in an ensemble of interacting nanostructures and is attributed to the sensitivity enhancement of a LSPR biosensor.[18,19,20] The specific nature of the field enhancement in a metallic nanostructure depends on intrinsic parameters, such as material, size, and shape, as well as extrinsic factors of the surrounding local media.[6,7,21] These LSPR devices can therefore serve as a transmission-based biosensor with extremely high sensitivity.[16] For example, it was shown that an extinction spectrum of the LSPR induced by silver nanoparticles is highly sensitive to the specific binding of anti-biotin to a biotinylated surface.[22] It was also reported that regularly distributed triangular nanoparticles are more sensitive than spherical colloidal nanoparticles due to the shape dependence of the plasmon resonance and the coupling effect between nanoparticles, so that an ensemble of periodic silver nanoparticles can be applied to a nanoscale optical biosensor.

The resonant field enhancement from periodic metal arrays is far greater than that of aperiodic arrays or randomly roughened metal surfaces.[23] Thus, the periodicity of an ensemble of nanostructures is an important parameter that needs to be considered. Suppose that we have well-separated and non-interacting nanostructures.

When the period is notably less than the wavelength of the incident light, electromagnetic coupling of individual nanostructures has prominent influence on the resonance condition. In general, two distinct types of interaction effects may occur in relation to the period. In a considerably short distance, short-range interactions between neighboring nanostructures induce near-field coupling that creates highly sensitive plasmons confined to metal boundaries. However, when the period exceeds the range of near-field coupling, far-field interactions prevail among nanostructure arrays, as have been elucidated using a dipole-dipole interaction model.[24] While an individual metallic nanostructure gives rise to dipole fields, induced dipoles oscillate resonantly in the neighboring nanostructures, leading to the formation of LSPs and local field enhancement. Using far-field interactions, metallic nanostructures can also be exploited as optical waveguides.[25]

Despite stronger field enhancement, near-field coupling configuration can suffer from worse sensing performance and more difficult implementation as a sensor, compared with a configuration based on far-field coupling. The near-field coupling generally shows complicated extinction spectra with multiple resonance peaks, which makes it difficult to detect the main resonance response to biological binding events linearly. In addition, the near-field coupling structure can be extremely sensitive to fabrication errors involved in realizing nanostructures with a very small period of a complicated profile. Consequently, we consider interacting nanostructures in the range of far-field coupling.

The goal of this study is to use nanowires to implement nanostructures for the simplicity of modeling and reliable fabrication and, furthermore, to understand relevant design issues to achieve maximal sensitivity enhancement as well as highly linear detection in sensing performance. For this purpose, we explore the profile dependence of optical extinction properties of excited LSP modes by introducing nanowire geometries of a T- and an inverse T-profile and the effect of other design parameters such as the nanowire period on the sensor performance. While a previous study showed extremely large field enhancement is possible with asymmetric nanowire profiles less than 50 nm in size,[26] such a structure is tremendously difficult to fabricate and to produce binding events on the sharp and slanted slope.

2. NUMERICAL MODEL

Suppose one-dimensional metallic nanowire gratings on a dielectric substrate as presented in Fig. 1. Silver or gold nanowires that are periodic in the x-axis are assumed to be aligned in the y-axis. The nanowires with a complex dielectric function are regularly patterned on a glass substrate ($n_s = 1.515$). The nanowire period (Λ) is considered in the range of 250 nm to 400 nm such that far-field dipolar interactions dominate. Assume that TM-polarized light, the electric field of which oscillates in parallel to the nanowire grating vector, is normally incident. Note also that both silver and gold were considered as nanowire material. Optical constants of silver and gold were taken from Ref. 27.
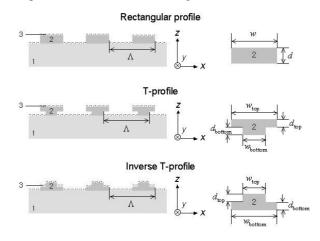

Figure 1. Cross-section of a nanowire-modified LSPR biosensor. Metallic nanowires with a period Λ are aligned in the y-axis. TM polarized light is normally incident on a glass substrate. Layer 1, 2, and 3 represent a glass substrate, silver or gold nanowires, and target analytes, respectively. For a rectangle, $w = 100$ nm and $d = 20$ nm; for a T, $w_{top} = 100$ nm, $w_{bottom} = 50$ nm, and $d_{top} = d_{bottom} = 10$ nm; for an inverse T, $w_{top} = 50$ nm, $w_{bottom} = 100$ nm, and $d_{top} = d_{bottom} = 10$ nm.

To describe the optical response of metallic nanowires, extinction spectra were calculated by rigorous coupled wave analysis (RCWA),[28,29] which has been successfully applied to explaining optical responses of nanostructures.[30,31] Our RCWA routine has been found to corroborate the experimental results of earlier studies using metallic nanostructures in the range of a few tens of nanometers in size,[32] offering an effective scheme to analyze optical properties of nanowires including extinction spectra.

Optical extinction is defined as $-\log(T)$, where T denotes transmittance as a function of the light wavelength. In order to quantify the sensitivity of the LSPR sensing configuration with respect to changes in the refractive index of the dielectric media surrounding metallic nanowires, target binding between biomolecules is modeled with a dielectric monolayer. Here, the refractive index change is induced by binding events of target analytes inside the flow channel and is assumed to represent the concentration change in binding events linearly. The thickness of this layer is assumed to be 3 nm based on the amplitude distribution of the excited plasmons that rapidly decreases outside the nanostructures. Note that the effect of LSP modes becomes insignificant if more than 3 nm away from the nanostructure surface for various cross-sections.[26] The monolayer covers the top surface of nanowires as well as the surface between nanowires on a glass substrate. The resonance wavelength shift is evaluated as the refractive index of the binding dielectric layer (n_d) increases from 1.0 to 1.5.

In our numerical model of one-dimensional metallic nanowires, we consider three different nanowire profiles: a rectangle, a T, or an inverse T as shown in Fig. 1, where w_{top} (w_{bottom}) denoting the width of the nanowire top (bottom) is either 100 nm or 50 nm. The nanowire depth d ($= d_{top} + d_{bottom}$) is fixed at 20 nm. A rectangular profile has the same width ($= 100$ nm) of the nanowire top and bottom. In other words, $w_{top} = 100$ nm, $w_{bottom} = 50$ nm, and $d_{top} = d_{bottom} = 10$ nm for a T-profile, and $w_{top} = 50$ nm, $w_{bottom} = 100$ nm, and $d_{top} = d_{bottom} = 10$ nm for an inverse T-profile. Consequently, T- and inverse T-profile nanowires take an equal volume if the period is identical.

3. RESULTS AND DISCUSSION

In Fig. 2, extinction properties have been calculated by varying periods, Λ, for (a) silver and (b) gold nanowire gratings with a rectangular profile at $w = 100$ nm and $d = 20$ nm. The resonance wavelength (λ_{LSPR}) and the width of the extinction peak represent the LSPR and the damping of LSPs, respectively. λ_{LSPR} blue-shifts (i.e. shifts toward a shorter wavelength) for both silver and gold nanowires, as Λ is decreased from 400 nm to 250 nm. This is in good agreement with an empirical report for orderly patterned nanostructure arrays at a period that is approximately half the λ_{LSPR}.[19] At nanowire periods in the range of 200 – 500 nm, radiative dipole interactions between nanowires as well as large retardation effects are deemed responsible for the blue shift.

Obviously, the dielectric function of a metallic nanostructure has a dominant effect on the resonance condition. The difference in the dielectric function causes λ_{LSPR} of gold nanowires to be located at longer wavelengths than that of silver. More specifically, as the imaginary part of the dielectric function of gold is larger than that of silver, the extinction of gold nanowires generally has a lower maximum value at resonance.
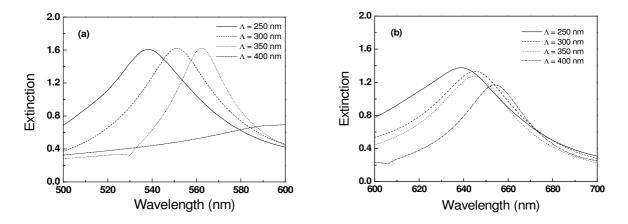

Figure 2. Extinction spectra of nanowire arrays with a rectangular profile assuming no analytes. For (a) silver and (b) gold nanowires, $\lambda_{LSPR} = 562$ nm (silver) vs. 645 nm (gold) at $\Lambda = 350$ nm.

For both silver and gold nanowires, the nanowire period for optimal biosensing was determined to be 350 nm since it provides relatively large extinction and narrow resonance width (full width at half maximum) than at other periods. In Fig. 2 (b), even though the extinction spectrum at Λ = 250 nm exhibits larger extinction, its resonance width is larger, which indicates poorer selectivity in sensing applications. As a result, Λ = 350 nm is employed for silver and gold nanowires in what follows, unless noted otherwise, in calculating the shift of λ_{LSPR} with the refractive index. As will be clear, the optimum period Λ = 350 nm is also valid for a T- and an inverse T- profile as well as a rectangular profile.
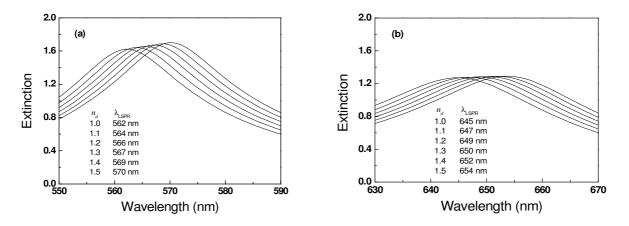

Figure 3. Extinction spectra of rectangular nanowires of (a) silver and (b) gold at Λ = 350 nm as n_d increases from 1.0 to 1.5.

As the refractive index of a dielectric binding layer increases from 1.0 to 1.5, λ_{LSPR} shifts to a longer wavelength (red-shift). For a rectangular profile, total spectral changes are 8 nm for silver nanowires and 9 nm for gold as depicted in Fig. 3. Linear regression analyses show that the shift is fairly linear over the whole range of refractive indices and that the refractive index sensitivities are 16.0 nm/RIU for silver and 17.4 nm/RIU for gold (RIU short for refractive index unit). R is the correlation coefficient that denotes the linearity obtainable in the sensor performance. R^2 for silver and gold nanowires of a rectangular profile is 0.994 and 0.997, respectively.
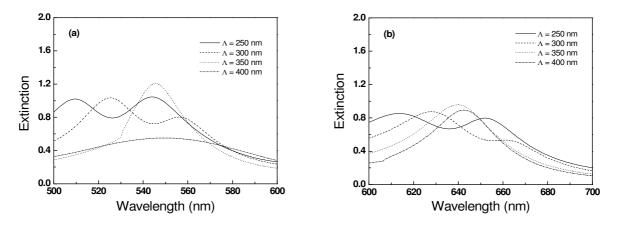

Figure 4. Extinction spectra of nanowire arrays with a T-profile assuming no analytes. For (a) silver and (b) gold nanowires, λ_{LSPR} = 546 nm (silver) vs. 640 nm (gold) at Λ = 350 nm.

In what follows, the effect of the nanowire profile on the sensitivity is estimated by comparing two different nanowire profiles, a T- and an inverse T-profile, with a rectangular profile. Figure 4 shows the extinction spectra at various periods (Λ = 250 nm - 400 nm) of silver and gold nanowires for a T-profile. Similar to the results of a rectangular profile in Fig.

2, the extinction spectra still have maximum values in $\lambda = 500 - 600$ nm for silver and in $\lambda = 600 - 700$ nm for gold. In particular, at $\Lambda = 250$ nm and 300 nm, both silver and gold nanowires of a T-profile show multiple extinction peaks.

These additional extinction peaks originate from the excitation of higher order harmonics of multipolar plasmon oscillations, induced by the complex nanowire profile. Since the optical near-field distribution around a nanostructure is affected by the order of excited multipolar plasmon modes, which modify optical properties of metallic nanowires intricately,[33] the extinction spectra also present a less linear sensitivity characteristic to binding biomolecular changes.
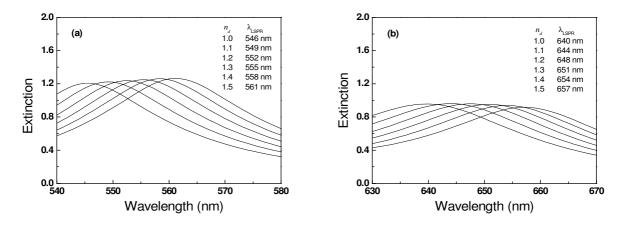

Figure 5. Extinction spectra of (a) silver and (b) gold nanowires of a T-profile at $\Lambda = 350$ nm as n_d increases from 1.0 to 1.5.

The extinction effects of the T-profile on the refractive index sensitivity are shown in Fig. 5 that represents extinction spectra and the change of an extinction peak with n_d. For silver nanowires, the resonance shift to an increase of n_d is completely linear with sensitivity equal to 30 nm/RIU. This is almost two times larger than in the case of a rectangular profile. Gold nanowires of a T-profile also exhibit improved sensitivity of 33.7 nm/RIU compared to rectangular gold nanowires at an identical period ($\Lambda = 350$ nm).
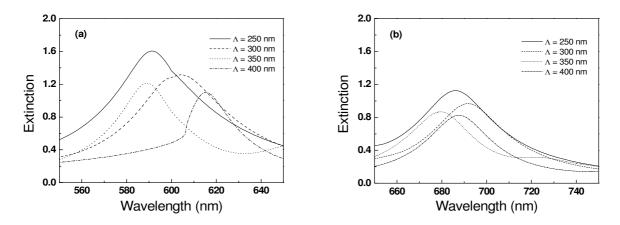

Figure 6. Extinction spectra of nanowire arrays with an inverse T-profile assuming no analytes. For (a) silver and (b) gold nanowires, $\lambda_{LSPR} = 589$ nm (silver) vs. 679 nm (gold) at $\Lambda = 350$ nm.

Secondly, an inverse T-profile has been calculated at various periods ($\Lambda = 250$ nm - 400 nm). The results are shown in Fig. 6 for silver and gold nanowires. The difference in the dielectric function between silver and gold leads to a larger extinction maximum and shorter resonance wavelength with silver than in the case of gold. Moreover, in extinction spectra at $\Lambda = 250$ nm and 300 nm, similar to a T-profile, secondary peaks originating from multipolar plasmon modes appear in the wavelength range $\lambda < \lambda_{LSPR}$ for both silver and gold nanowires. At this period, the refractive index sensitivity cannot be identified as linear, as the higher-order terms significantly influence the optical performance of a

LSPR biosensor. Sensitivity improvement is also observed at Λ = 350 nm for an inverse T-profile. In Fig. 7, λ_{LSPR} shows red-shift as n_d increases with the sensitivity of 27.7 nm/RIU for both silver and gold nanowires, a largely enhanced value compared to that of a rectangular profile.
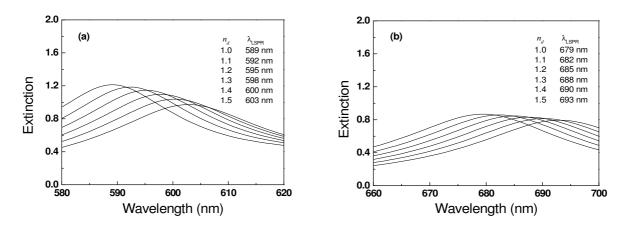

Figure 7. Extinction spectra of (a) silver and (b) gold nanowires of an inverse T-profile at Λ = 350 nm as n_d increases from 1.0 to 1.5 (increase in the direction of arrow).

As listed in Table 1, it is apparent that the nanowire profile affects the LSPR sensor performance, the sensitivity in particular, tremendously. For instance, the field inside a circular nanostructure, which is highly symmetric, becomes almost homogeneous and the field amplitude decays drastically outside the nanostructure.[26] It was also found that the field is highly heterogeneous for non-rectangular profiles and that especially at main resonance with a maximum extinction value, the field amplitude takes large values at corners. In other words, the field amplitude is enhanced rapidly as the profile of a nanostructure becomes more complex and asymmetric.

Silver	Sensitivity	Linearity
Rectangle	16.0 nm/RIU	0.994
T	30.0 nm/RIU	1.000
Inverse T	27.7 nm/RIU	0.998

Gold	Sensitivity	Linearity
Rectangle	17.4 nm/RIU	0.997
T	33.7 nm/RIU	0.997
Inverse T	27.7 nm/RIU	0.998

Table 1. Calculated sensitivity and square of correlation coefficient (R^2) for silver and gold nanowires of different profiles at Λ = 350 nm.

This plasmonic interpretation based on the corner effect and the field enhancement for a non-rectangular profile can be applied to analyzing our results. As a T- or an inverse T-profile mimics a trapezoid that is an intermediate state between a rectangle and a triangle, the two profiles present larger field amplitude enhancement with more strongly excited LSPs and induce higher sensitivity, associated with less symmetry than a rectangular profile. Furthermore, the two profiles provide a more feasible structure with enhanced customizability than a triangular or an inverse triangular profile.

In our results, a T-profile on the whole shows better sensitivity to the change of refractive indices than an inverse T-profile. To qualitatively understand the difference in the performance of the two profiles, suppose approximating a T-profile as an inverted trapezoid and an inverse T-profile as a trapezoid, respectively, such that they occupy an equal volume. The corner effect stipulates that when the resonance occurs, extremely strong fields are excited in the vicinity of corners in nanostructures. For an inverted trapezoid, fields are enhanced mainly at two vertices on the top, where the binding events of target analytes occur. In contrast, the field enhancement for a trapezoid structure occurs at both end-points on the bottom which is relatively far from the layer of target analytes. In consequence, a closer distance between highly enhanced fields and the binding events results in better sensitivity performance for nanowires of a T-profile.

4. CONCLUSIONS

In this study, we have calculated optical extinction properties of silver and gold nanowires on a dielectric substrate using RCWA. Our results show that the resonance spectrum strongly depends on the nanowire period and profile. For nanowire periods in the far-field coupling, dipole interactions between metallic nanowires result in the blue-shift of λ_{LSPR} as Λ varies from 400 nm to 250 nm. The complexity of the LSPR extinction spectrum has been discussed for silver and gold nanowires with a T- and an inverse T-profile.

Our results indicate that the extinction spectra of the LSPR sensor based on metallic nanowires are fairly linear and significantly sensitive to changes of refractive indices of dielectric binding media if design parameters are properly optimized. In our investigation, $\Lambda = 350$ nm achieves both high extinction peak and narrow resonance width for the profiles considered. For both silver and gold nanowires, the T- and the inverse T-profiles exhibit better sensitivity than a rectangular profile. In particular, a T-profile presents the highest sensitivity of 33.7 nm/RIU for gold and 30.0 nm/RIU for silver. This study is expected to provide a basis to implement feasible structures as a LSPR biosensor based on metallic nanowires with excellent sensing performance.

ACKNOWLEDGEMENTS

REFERENCES

1. H. Raether, *Surface Plasmons on Smooth and Rough Surfaces and on Gratings*, Springer-Verlag, Berlin (1988).
2. B. Liedberg, C. Nylanderm, and I. Lundström, "Surface plasmon resonance for gas detection and biosensing," Sens. Actuators **4**, 299-304 (1983).
3. K. Matsubara, S. Kawata, and S. Minami, "Optical chemical sensor based on surface plasmon measurement," Appl. Opt. **27**, 1160-1163 (1988).
4. J. Homola, S. S. Yee, and G. Gauglitz, "Surface plasmon resonance sensors: review," Sens. Actuators B **54**, 3-15 (1999).
5. M. J. O'BrienII, V. H. Pérez-Luna, S. R. J. Brueck, and G. P. López, "A surface plasmon resonance array biosensor based on spectroscopic imaging," Biosens. Bioelectron. **16**, 97-108 (2001).
6. U. Kreibig and M. Vollmer, *Optical Properties of Metal Clusters*, Springer-Verlag, Berlin (1995).
7. P. Mulvaney, "Surface plasmon spectroscopy of nanosized metal particles," Langmuir **12**, 788-800 (1996).
8. T. R. Jensen, M. D. Malinsky, C. L. Haynes, and R. P. Van Duyne, "Nanosphere lithography: Tunable localized surface plasmon resonance spectra of silver nanoparticles," J. Phys. Chem. B **104**, 10549-10556 (2000).
9. T. Okamoto, I. Yamaguchi, and T. Kobayashi, "Local plasmon sensor with gold colloid monolayers deposited upon glass substrates," Opt. Lett. **25**, 372-374 (2000).
10. G. Kalyuzhny, M. A. Schneeweiss, A. Shanzer, A. Vaskevich, and I. Rubinstein, "Differential plasmon spectroscopy as a tool for monitoring molecular binding to ultrathin gold films," J. Am. Chem. Soc. **123**, 3177-3178 (2001).
11. L. A. Lyon, D. J. Pena, and M. J. Natan, "Surface plasmon resonance of Au colloid-modified Au films: Particle size dependence," J. Phys. Chem. B **103**, 5826-5831 (1999).
12. E. Hutter, S. Cha, J-F. Liu, J. Park, J. Yi, J. H. Fendler, and D. Roy, "Role of substrate metal in gold nanoparticle enhanced surface plasmon resonance imaging," J. Phys. Chem. B **105**, 8-12 (2001).

13. L. He, M. D. Musick, S. R. Nicewarner, F. G. Salinas, S. J. Benkovic, M. J. Natan, and C. D. Keating, "Colloidal Au-enhanced surface plasmon resonance for ultrasensitive detection of DNA hybridization," J. Am. Chem. Soc. **122**, 9071-9077 (2000).

14. K. M. Byun, S. J. Kim, and D. Kim, "Design study of highly sensitive nanowire-enhanced surface plasmon resonance biosensors using rigorous coupled wave analysis," Opt. Express **13**, 3737-3742 (2005).

15. T. Kume, N. Nakagawa, S. Hayashi, and K. Yamamoto, "Interaction between localized and propagating surface plasmons: Ag fine particles on Al surface," Solid State Commun. **93**, 171-175 (1995).

16. A. D. McFarland and R. P. Van Duyne, "Single silver nanoparticles as real-time optical sensors with zeptomole sensitivity," Nano Lett. **3**, 1057-1062 (2003).

17. J. J. Mock, D. R. Smith, and S. Schultz, "Local refractive index dependence of plasmon resonance spectra from individual nanoparticles," Nano Lett. **3**, 485-491 (2003).

18. E. Hutter and J. H. Fendler, "Exploitation of localized surface plasmon resonance," Adv. Mater. **16**, 1685-1706 (2004).

19. C. L. Haynes, A. D. McFarland, L. Zhao, R. P. Van Duyne, G. C. Schatz, L. Gunnarsson, J. Prikulis, B. Kasemo, and M. Käll, "Nanoparticle optics: The importance of radiative dipole coupling in two-dimensional nanoparticle arrays," J. Phys. Chem. B **107**, 7337-7342 (2003).

20. S. Enoch, R. Quidant, and G. Badenes, "Optical sensing based on plasmon coupling in nanoparticle arrays," Opt. Express **12**, 3422-3427 (2004).

21. C. Sönnichsen, T. Franzl, T. Wilk, G. von Plessen, J. Feldmann, O. Wilson, and P. Mulvaney, "Drastic reduction of plasmon damping in gold nanorods," Phys. Rev. Lett. **88**, 077402 (2002).

22. A. J. Haes and R. P. Van Duyne, "A nanoscale optical biosensor: Sensitivity and selectivity of an approach based on the localized surface plasmon resonance spectroscopy of triangular silver nanoparticles," J. Am. Chem. Soc. **124**, 10596-10604 (2002).

23. D. A. Genov, A. K. Sarychev, V. M. Shalaev, and A. Wei, "Resonant field enhancements from metal nanoparticle arrays," Nano Lett. **4**, 153-158 (2004).

24. W. Rechberger, A. Hohenau, A. Leitner, J. R. Krenn, B. Lamprecht, and F. R. Aussenegg, "Optical properties of two interacting gold nanoparticles," Opt. Commun. **220**, 137-141 (2003).

25. S. A. Maier, M. L. Brongersma, P. G. Kik, S. Meltzer, A. A. G. Requicha, and H. A. Atwater, "Plasmonics – A route to nanoscale optical devices," Adv. Mater. **13**, 1501-1505 (2001).

26. J. P. Kottmann, O. J. F. Martin, D. R. Smith, and S. Schultz, "Plasmon resonances of silver nanowires with a nonregular cross section," Phys. Rev. B **64**, 235402 (2001).

27. E. D. Palik, *Handbook of Optical Constants of Solids*, Academic Press, Orlando, FL (1985).

28. M. G. Moharam and T. K. Gaylord, "Diffraction analysis of dielectric surface-relief gratings," J. Opt. Soc. Am. **72**, 1385-1392 (1982).

29. M. G. Moharam and T. K. Gaylord, "Rigorous coupled-wave analysis of metallic surface-relief gratings," J. Opt. Soc. Am. A **3**, 1780-1787 (1986).

30. J. Lermé, "Introduction of quantum finite-size effects in the Mie's theory for a multilayered metal sphere in the dipolar approximation: application to free and matrix-embedded noble metal clusters," Eur. Phys. J. D **10**, 265-277 (2000).

31. E. Moreno, D. Erni, C. Hafner, and R. Vahldieck, "Multiple multipole method with automatic multipole setting applied to the simulation of surface plasmons in metallic nanostructures," J. Am. Opt. Soc. A **19**, 101-111 (2002).

32. K. M. Byun, D. Kim, and S. J. Kim, "Investigation of the sensitivity enhancement of nanoparticle-based surface plasmon resonance biosensors using rigorous coupled-wave analysis," in Plasmonics in Biology and Medicine II, T. Vo-Dinh, J. R. Lakowicz, Z. K. Gryczynski, eds., Proc SPIE **5703**, 61-70 (2005).

33. J. R. Krenn, G. Schider, W. Rechberger, B. Lamprecht, A. Leiter, F. R. Aussenegg, and J. C. Weeber, "Design of multipolar plasmon excitations in silver nanoparticles," Appl. Phys. Lett. **77**, 3379-3381 (2000).